

**A MODEL FOR FUEL OXIDATION AND DIFFUSION-BASED FISSION PRODUCT RELEASE
UNDER SEVERE NUCLEAR REACTOR ACCIDENT CONDITIONS**

P.L. PURDY, B.J. LEWIS AND W.S. ANDREWS
Royal Military College of Canada
Department of Chemistry and Chemical Engineering
Kingston, Ontario, CANADA K7K 5L0

D.S. COX
Atomic Energy of Canada Limited, Research Company
Chalk River Laboratories
Chalk River, Ontario, CANADA K0J 1J0

F.C. IGLESIAS
Ontario Hydro
Reactor Safety and Operational Analysis Department
700 University Avenue
Toronto, Ontario, CANADA M5G 1X6

ABSTRACT

A fuel oxidation and diffusion-based fission product release model has been developed from the recent analysis of ^{134}Cs data from a number of experiments performed at the Chalk River Laboratories (CRL). The release model was based on data from six tests in the Hot Cell Experiment (HCE2). These tests were conducted in steam from 1354 to 1651°C, and contained fuel samples of either bare fuel fragments or Zircaloy-clad mini-elements. The fraction of fission products trapped in the fuel was also determined from additional tests in the Hot Cell Experiments (HCE1 and HCE2), and the Universal Cell Experiment (UCE12). The model has been validated against eight other tests not used in the model development, resulting in a value of 0.11 for the mean absolute difference from experiment. The present treatment has also been compared to the ORNL simple diffusion model and the empirically based CORSOR-M model with resultant mean absolute difference values of 0.24 and 0.17, respectively, for the same validation set.

1. INTRODUCTION

Within the reactor core under accident conditions, high temperatures will accelerate thermal diffusion of the fission products from the UO_2 fuel. In addition, hydrogen will be generated at high temperatures by the steam oxidation of the core materials, which will alter the oxygen potential within the core. Annealing experiments on bare fuel specimens (fuel fragments) of uranium dioxide have been recently performed at the Chalk River Laboratories (CRL) to investigate the effects of fuel oxidation on the release kinetics of volatile fission products^{1,2}. Even in breached fuel rods, the Zircaloy cladding can provide both a physical and chemical barrier that can delay or reduce the release of fission products. This effect has been demonstrated in CRL tests with short-length fuel elements (mini-elements)²⁻⁴. The cladding can provide a sink for oxygen, and a source of hydrogen, due to the metal-water reaction at high temperature, thus retarding the oxidation of the fuel and release of fission products⁵.

In this paper, it is shown that a generalized diffusion-based model can be used to predict the fission product release kinetics based on an integral-time transformation. Experimental data from the CRL program are used to develop a physically-based model for predicting the release of fission product ^{134}Cs from UO_2 fuel at high temperatures in both reducing ($\text{Ar}/2\%\text{-H}_2$) and oxidizing (steam) atmospheres. The model accounts for thermal diffusion, enhanced release during temperature ramps, diffusion due to oxidation of the fuel (with or without the presence of Zircaloy cladding) and a trapped inventory dependent on fuel characteristics. The model is further applied to a total of 17 CRL experiments and compared to predictions from both the CORSOR-M kinetic model and the ORNL diffusion model.

2. EXPERIMENTAL RESULTS AND ANALYSIS

2.1 CRL HCE2 Experiments

An analysis of six HCE2 experiments, performed at CRL, is considered in the present work. Four of these experiments represent new data from that reported in Refs. 6 and 7. The tests were conducted on both bare UO_2 fragments (CF1, CF2 and CF3) and short-length mini-elements (CM1, CM2 and CM6). All fuel specimens were obtained by cutting a section of a single spent fuel element of a CANDU-type design. The mini-elements also contained loose-fitting end-caps (see Ref. 7). The details of the experiments are briefly summarized in Table 1.

Each fuel specimen was introduced into a flowing mixture of $\text{Ar}/2\%\text{-H}_2$ (400 ml/min at STP) and ramped to a given temperature plateau of: 1360°C (CF2, CM2), 1500°C (CF3, CM6) and 1645°C (CF1, CM1). After the temperature plateau had been reached, the fuel was immediately exposed to an oxidizing mixture of steam (60 g/h) and argon (100 ml/min at STP). The oxygen partial pressure of the atmospheric composition upstream and downstream from the fuel location were continuously monitored with yttria-stabilized zirconia oxygen sensors⁸. Fission products released from the fuel specimens were swept away such that a gamma-ray spectrometer, collimated at the sample location, provided information on the kinetic release behaviour.

The experiments were carried out under similar atmospheric and temperature conditions so that a direct comparison could be made between the two different fuel types. Hydrogen production from the Zircaloy-steam reaction will reduce the oxygen potential of the atmosphere, and thereby inhibit the fuel oxidation kinetics and resultant fission product release. These tests therefore provide a means to quantify the physical and chemical influence of the Zircaloy cladding on the release behaviour. The release kinetics of ^{134}Cs for experiments CF3 and CM6, representing the two types of test specimens, are shown in Figs. 1(a) and (b), respectively. A delay in the release behaviour is typically observed in the mini-element tests compared to that of the bare fuel fragments. This effect is mathematically modelled in Section 2.2.

2.2 Model Development

It has been suggested earlier that the cesium release follows a two-stage process^{6,7}. However, there is no physical explanation to warrant a change in kinetics (i.e., no phase change occurs in the fluorite lattice structure below a stoichiometry deviation value of $x = 0.25$ in UO_{2+x} , and any release by grain growth is limited with a pinning of the grain boundaries by the fission product bubbles)⁹. In the earlier treatment, the diffusion-based release became more restricted with increasing time due to the use of a Taylor series approximation for the fractional release representation^{6,7}. As shown in the present work, this problem can be overcome with a more generalized numerical treatment. An integral-time transformation can be used for the diffusion equation to account for a changing diffusivity with temperature and stoichiometry deviation^{10,11}. Consequently, the generalized release fraction is given by^{6,7}:

$$F = (1 - g_0 - \zeta) F_D(\tau) + g_0, \quad (1)$$

where g_0 accounts for the fuel-to-clad gap release fraction for mini-element tests (see Section 2.4), and ζ is the fraction of the fission product inventory trapped in the fuel porosity. The function $F_D(\tau)$ is given by the transformed Booth relation^{10,11}:

$$F_D = 6\sqrt{\frac{\tau}{\pi}} - 3\tau, \quad \text{for } \tau \leq 0.1, \quad (2)$$

$$F_D = 1 - \frac{6}{\pi^2} \exp(-\pi^2 \tau), \quad \text{for } \tau > 0.1. \quad (3)$$

The dimensionless variable τ is evaluated from the integral relation

$$\tau = \int_0^t D'(t) dt \approx \sum_0^t D'(t) \Delta t, \quad (4)$$

where $D' = D/a^2$, D is the diffusion coefficient and a is the grain radius. Equation (4) accounts for the time-variable diffusion coefficient, D , that depends directly on the stoichiometry deviation, x , and temperature, T . The grain radius, a , is typically constant during the anneal since the grain boundaries are pinned by the fission product bubbles. As shown in the second expression of Eq. (4), the integral can be replaced by a rectangular-integration rule where $D'(t)$ is considered to be constant over a small time step Δt .

For the calculation of Eq. (1), the fission product diffusivity must be evaluated for hyperstoichiometric fuel. The experimental work of Matzke indicates that xenon diffusion occurs at a neutral tri-vacancy site in the uranium dioxide matrix¹². The energy minimization calculations of Grimes and Catlow provide further evidence for this mechanism, where it is predicted that this site is stable for xenon¹³. The same calculations also suggest that the most favourable solution site for both xenon and cesium in hyperstoichiometric urania (UO_{2+x}) is the uranium vacancy. This finding is in agreement with other experimental and theoretical work for the calculation of the rare gas diffusion coefficient¹⁴⁻¹⁶. For instance, the diffusion coefficient, D (in m^2/s), as a function of the temperature, T (in K), and stoichiometry deviation, x , can be given by the composite expression^{6,7,15,16}:

$$D = D(T) + D(x, T), \quad (5)$$

where the intrinsic diffusion component is given by

$$D(T) = 7.6 \times 10^{-10} \exp\left(\frac{-7.0 \times 10^4}{RT}\right), \quad (6)$$

and the enhanced uranium vacancy production term is

$$D(x, T) = 4s^2 j_v V_U. \quad (7)$$

In Eqs. (6) and (7), R is the ideal gas constant (1.987 cal/mol·K), s is the atomic jump distance (3×10^{-10} cm) and $j_v = 10^{13} \exp(-5.52 \times 10^4 / RT)$ (s^{-1}) is the vacancy jump rate. The uranium vacancy concentration, V_U , is defined by¹⁵

$$V_U = \frac{Sx^2}{F_0^2} \left(\frac{1}{2} + \frac{F_0}{x^2} + \frac{1}{2} \sqrt{1 + \frac{4F_0}{x^2}} \right), \quad (8)$$

where the parameters $S = \exp(-1.47 \times 10^5 / RT)$ and $F_0 = \exp(-1.13 \times 10^4 / RT)$ correspond to the Schottky and Frenkel defect, respectively. For most values of x and T under consideration, the condition $x^2 \gg 4F_0$ will hold and V_U reduces to

$$V_U \approx \frac{Sx^2}{F_0^2}, \quad \text{for } x^2 \gg 4F_0. \quad (9)$$

Consequently, Eq. (7) can be written in a much simpler form:

$$D(x, T) = D_{0ox} x^2 \exp\left(\frac{-Q_{ox}}{RT}\right), \quad \text{for } x^2 \gg 4F_0, \quad (10)$$

where D_{0ox} and Q_{ox} are constants that can be obtained in the present analysis. With oxidized fuel, one generally finds that $D(x, T) \gg D(T)$ in Eq. (5).

Determination of the diffusion coefficient, $D(x, T)$, requires knowledge of the stoichiometry deviation. The first step is to evaluate the oxygen partial pressure, p_{O_2} (in atm), of the atmosphere surrounding the fuel. This can be achieved using a Newton's iterative method for the transcendental expression^{17,18}:

$$K \sqrt{p_{O_2}} \left[\left(\frac{Q_a}{2} - 1 \right) + \left(\frac{Q_a}{2} + 1 \right) \left(\frac{p_{O_2}}{p_t} \right) \right] = 1 - (Q_a + 1) \left(\frac{p_{O_2}}{p_t} \right). \quad (11)$$

Here, p_t is the total system pressure in atmospheres and $K = \exp(-\Delta G^0/RT)$, where $\Delta G^0 = -59.9 + 13.8(T/10^3)$ kcal/mol. The parameter Q_a is the hydrogen-to-oxygen atom ratio for a bulk atmosphere that contains a steam/hydrogen mixture⁷:

$$Q_a = 2 \left(1 + \frac{n_{H_2}}{n_{H_2O}} \right) = 2 \left(1 + \frac{\frac{1}{2}R_{H_2}}{f_g R_{H_2O} - \frac{1}{2}R_{H_2}} \right), \quad (12)$$

where (n_{H_2}/n_{H_2O}) is the molar ratio for the gas mixture, R_{H_2O} is the rate of steam input into the experiment (in mol/s) and R_{H_2} is the hydrogen production rate (mol/s) arising from the Zircaloy/steam reaction. The parameter f_g accounts for mass transfer of the steam into the fuel-to-clad gap of a breached fuel rod (i.e., loose-fitting end-caps were used in the CRL mini-element tests). Oxidation of the fuel can then be quantified by equating the oxygen potential in the atmosphere (calculated from Eq. (11)) to that of the solid fuel. Hence, the equilibrium stoichiometry deviation, x_e , can be solved from the Blackburn thermochemical model for the oxygen in the fuel, using a Newton's iterative method^{17,19}:

$$P_{O_2} = \left[\left(\frac{x_e(2+x_e)}{(1-x_e)} \right)^2 k \right], \quad (13)$$

where k is an empirical constant and $\ln(k) = 108x_e^2 - 32700/T + 9.92$. The fuel oxidation kinetics are governed by a surface-exchange reaction at the solid/gas interface defined by²⁰⁻²³

$$\frac{dx}{dt} = \alpha [x_e - x(t)](S/V), \quad (14)$$

where S/V (in m^{-1}) is the surface-to-volume ratio and $\alpha = 0.365 \exp(-23500/T)$ (m/s) is the oxygen surface-exchange coefficient as experimentally determined by Cox et al. at 1 atm^{9,22}. Using a Taylor series approximation, $x(t)$ can be evaluated from one time step to the next as

$$x(t + \delta t) = x(t) + \frac{dx}{dt} \delta t, \quad (15)$$

where dx/dt is given by Eq. (14).

During the initial temperature ramp, the fuel specimens experienced a slightly reducing atmosphere, in which the intrinsic diffusion coefficient in Eq. (6) should apply. However, this diffusivity results in a significant underprediction of the observed release behaviour. This finding may result from the fact that Eq. (6) is derived from isothermal experiments²⁴. Preliminary tests at CRL demonstrate a release dependence on the temperature ramp rate (dT/dt). In addition, Une and Kashibe have reported a predominant release from the grain boundary inventory during heating, where the critical temperature for the onset of this process was lower with increased fuel burnup²⁵. The present analysis incorporates this effect into a temperature ramp enhancement factor, E_{tr} , where Eq. (5) is replaced by:

$$D = (1 + E_{tr} \frac{dT}{dt}) D(T) + D(x, T). \quad (16)$$

2.3 Fuel Fragment Analysis

The fuel oxidation model can be directly tested against the measured stoichiometry deviation for the fuel fragment experiments. Using the measured oxygen partial pressure in the Blackburn model of Eq. (13), the equilibrium stoichiometry deviation, x_e , can be evaluated. A further calculation can also be performed by equating the oxygen potential in the solid, using the Blackburn model (Eq. (13)), to the oxygen potential for a pure steam atmosphere (i.e., $Q_a = 2$ in Eq. (12)). As shown in Table 1, these calculations are in good agreement with the measured end-state stoichiometry deviation. Using the calculation of x_e in Table 1 (model), the fuel oxidation kinetics can be predicted with Eqs. (14) and (15). Following the analysis of Ref. (7), it is assumed that the surface-to-volume ratio, (S/V), is three times the geometrical one to include the effects of surface roughness and fuel cracking (Table 1). The geometrical ratio is based on a calculation that the fuel fragments are perfect cubes. A comparison of the predicted and measured fuel oxidation kinetics is shown for the CF3 test in Fig. 1(c), which is representative of the other fragment tests.

With a knowledge of the fuel oxidation kinetics, the release behaviour can be evaluated. The cesium release can be modelled with Eqs. (1) through (4) and the diffusivity of (16), and using the stoichiometry deviation curves. The grain radius is fixed as $a = 3.5 \mu\text{m}$ for the peripheral fragments (see Table 1). For the present analysis, the trapped fraction, ζ , was also fixed to a value of one minus the measured (end-of-test) release fraction. The fitting parameters of the model are the constants D_{ox} and Q_{ox} for the diffusion coefficient (Eq. (10)) and the temperature ramp enhancement factor, E_{tr} (Eq. (16)). These parameters were fit simultaneously to all of the release data (including the mini-element tests - see Section 2.4) using a Marquardt-Levenberg algorithm²⁶. The fitting parameters are listed in Table 1. As represented in Fig. 1(a), the fission product release model is in good agreement with the measured results from the fuel fragment tests.

2.4 Mini-Element Analysis

The mini-element tests were conducted under the same conditions of temperature and atmosphere (steam) as the fuel fragment tests, except that the fuel specimens were clad in Zircaloy-4 (with end-caps). With this addition, the oxygen potential was continuously changing as a consequence of hydrogen production from the Zircaloy/steam reaction at high temperature. The fuel oxidation kinetics could not be instantaneously measured in these experiments because of the complicating effect of the Zircaloy/steam reaction. However, since all Zircaloy was converted to zirconium dioxide by the end of each test, the final weight gain for the fuel could be estimated from the oxygen partial pressure measurements. Therefore, the fuel oxidation could be tested against a measured end-state value of x . The effect of changing oxygen potential on the fuel oxidation kinetics can be evaluated from Eqs. (11) and (12), with the measured hydrogen production rates (see Fig. 1(d)) and steam input rates. Good agreement with the measured end-state values of x was obtained with a fitted value of $f_g = 20\%$ for all experiments, which accounts for the mass transfer of steam into the fuel-to-clad gap through the loose-fitting end-caps. It was further assumed that only pure steam was present in the gap following complete oxidation of the end-caps and sheath. At this time, external spigots on the end-caps had not completely oxidized. As shown in Table 1, the end-state oxidation was predicted to within 17% of the measured weight gain. The measured hydrogen production rate from the Zircaloy/steam reaction is shown in Fig. 1(d) where the pure steam assumption is implemented at a value for the hydrogen production rate of $6 \times 10^{-6} \text{ mol/s}$. This value of the hydrogen production rate was determined by employing parabolic kinetics to predict the Zircaloy oxidation process for the CM2 experiment using the coefficients of Pawel et al.^{7,28,29}. The predicted oxidation kinetics for the mini-element test CM6 are shown in Fig. 1(b).

In a similar analysis, the fission product release can be calculated using the predicted stoichiometry deviation kinetics. Here the diffusion coefficient parameters, D_{ox} , Q_{ox} and E_{tr} , were simultaneously fit to the release data from all tests (i.e., fuel fragments and mini-elements). The parameter ζ was again fixed to an estimated value

of 15% for all mini-element tests. The grain radius was set to the volumetrically-averaged value for the fuel pellet (i.e., 6.5 μm) as the temperature profile was uniform across the test specimen. Inspection of Figs. 1(a) and (b) shows that the release fraction at the start of the steam period is typically 15% larger for the mini-element compared to that of the fuel fragment. This additional source may result from a volatilization of the cesium that was originally deposited on the internal cladding surfaces during irradiation or from the specific surface condition of the fuel after irradiation. This value also accounts for differences in the available grain-boundary inventories (between the peripheral fragment and fuel pellet) that are additionally released with fuel cracking²⁷. To incorporate these effects into the present model, the fuel-to-clad gap parameter, g_0 , was set to 15% at the time when the volatilization temperature of cesium is reached (671°C). Note also that this parameter was necessary since limited release data was available during the temperature ramp as a result of the experimental setup.

As represented in Fig. 1(b) the release predictions are in good agreement with experiment, although these predictions are less precise than for those of the (small) fuel fragments (compare with Fig. 1(a)). This result is expected since the mini-element calculations are more complex because of the presence of the Zircaloy cladding barrier, which leads to a changing oxygen potential and a reduced mass transfer into the fuel-to-clad gap. Thus, uncertainties arise since the oxygen potential is based only on a point-kinetic model, as evaluated from the bulk stream properties using a single factor (for all tests) to account for steam transfer into the gap (f_g). The mini-elements also have a distribution of grain sizes compared to that of the (peripheral) fuel fragments; i.e., a further approximation is invoked by modelling the grain size with a single (volumetrically-averaged) value for the pellet. Fission product transport in the gap has also been neglected, although at high temperature conditions, any delay in the gap is considered to be small⁷.

2.5 Trapped Inventory Correlation

In order to extend the model for a more general analysis, a correlation was developed for the trapped fraction, ζ . If it is assumed that the trapped inventory results from a holdup in the intergranular bubbles⁶, this parameter can then be defined as the ratio of the number of fission product atoms on the grain boundary to the number in the grain volume³⁰:

$$\zeta = \frac{N_g \cdot 4\pi a^2}{N_f \cdot \frac{4}{3}\pi a^3}, \quad (17)$$

where N_g is the number of gas atoms trapped in bubbles per unit area of grain boundary and N_f is the number of gas atoms produced during irradiation per unit volume of fuel. Since N_g is dependent on temperature, and N_f is proportional to fuel burnup, the trapped fraction can be defined as:

$$\zeta = \frac{f(T)}{a \cdot BU}, \quad (18)$$

where a is the grain radius (in μm) and BU is the burnup (in MWh/kgU). To determine the temperature-dependent function, $f(T)$, the measured ζ values from 12 CRL tests (see Table 2) were multiplied by the grain radii and burnup. These results were then plotted versus temperature as shown in Fig. 2(a). Within the scatter of the resultant plot, no temperature dependence is apparent and a constant value of $f(T) = 300 \mu\text{m} \cdot \text{MWh/kgU}$ is fitted through the data. The quantity N_g is equal to the number of bubbles per unit area of grain boundary times the number of gas atoms in a bubble (m). Hence, the temperature dependence can be evaluated from the equation of state and a mechanical force balance for the bubble in which³¹

$$m = \left(\frac{4\pi R^2}{3} \right) \left(\frac{2\gamma}{R} + \sigma \right) \left(\frac{1}{kT} \right), \quad (19)$$

where R is the bubble radius, γ is the surface tension of the solid, σ is the hydrostatic stress and k is Boltzmann's constant. Thus, $f(T)$ is inversely proportional to the temperature. Since this trend is not apparent in Fig. 2(a), a more complex mechanism is presumably governing the trapped inventory. It is important to realize, however, that the trapped fraction, ζ , is typically less than 20%. Table 2 and Fig. 2(b) show the predictions of the present correlation versus the measured data. As seen in Fig. 2(b), the predictions deviate by up to a factor of 3. No trend, however, is observed from the line of perfect correlation within the groupings of the given data set. Figures 2(c) and (d) represent release calculations with the present model, using the correlation for ζ . As can be seen from these plots, the release kinetics are well predicted during the tests, but a poorer prediction results at the end of the tests due to the trapped fraction calculation.

3. MODEL APPLICATION

3.1 Comparison to Experiment

Using the trapped fraction correlation, the present analysis was applied to a validation set of eight experiments that had not been used in developing any portion of the model (footnote (a) in Table 2). The same diffusion coefficient was used for all experiments (see Table 1). A constant value for the surface-to-volume ratio of three times the geometric value was also assumed. As discussed in Section 2.4, a value of $f_g = 20\%$ was used for all Zr-clad experiments to model the fraction of steam into the fuel-to-clad gap. In addition, a pure steam assumption was employed for the mini-elements whenever the hydrogen production rate was below 6×10^{-6} mol/s. The only variables in the calculation were the test conditions themselves. The specimens were characterized by a volumetrically-averaged grain size, the burnup and a geometric surface-to-volume ratio. The changing experimental conditions included the temperature, temperature ramp rate and oxygen potential of the atmosphere. The environment (argon, hydrogen, steam) and the presence of Zircaloy cladding were therefore taken into account through the oxygen potential calculation.

Figure 3 shows the model comparison (with stoichiometry deviation for steam tests) for 4 of the 8 validation tests. The intrinsic diffusion coefficient, along with the temperature-ramp factor, are confirmed by the mini-element tests (Figs. 3(a) and (b)) conducted in an atmosphere of purified argon. The parameter, g_0 , was set to zero for these tests, since the specimens came from a different fuel rod. Figures 3(c) and (d) provide an assessment of the fuel oxidation and release model. The test in Fig. 3(c) is slightly underpredicted by the model, although the fuel fragment had broken up into several pieces during the test (i.e., an increase in the release of Ce was measured during the test)¹. This would have resulted in an increased surface-to-volume ratio which was not considered in the present calculation. In Fig. 3(d), the model slightly overpredicts the release when steam is initially introduced into the system. This result may be attributed to a slight overprediction of the fuel oxidation kinetics with the Blackburn methodology.

In order to quantify the release fraction prediction from the present treatment, the mean absolute difference between the model and experiment was evaluated from all of the data points within the validation set. A mean absolute difference of 0.11 was obtained for the release fraction, which provides a measure of accuracy for the model prediction.

3.2 Comparison to Other Models

The present model can be compared to other models currently employed in reactor accident analysis. The CORSOR-M model³² and the ORNL diffusion model³³ were run for the same experiments as the present calculation. The CORSOR-M and ORNL predictions are also shown in Figs. 1, 2 and 3, i.e., the present model typically predicts the release fraction more accurately than the other models. For instance, the mean absolute deviation for these models was 0.17 (CORSOR-M) and 0.24 (ORNL) (as compared to a value of 0.11 for the present model). Thus, the present model is able to better predict the release fraction by up to a factor of 2.

4. CONCLUSIONS

1. An analytical model has been developed to describe the release behaviour of fission product cesium from uranium dioxide fuel during severe reactor accident conditions. In the present framework, the fission product release kinetics are based on the state of fuel oxidation, in accordance with a generalized diffusion-based approach. The fuel oxidation kinetics are detailed by a surface-exchange reaction at the fuel/steam interface. The effect of a changing oxygen potential in the atmosphere (due to Zircaloy/steam reaction) is explicitly treated in the model.
2. The model is based on the recent CRL HCE2 tests, conducted in a steam atmosphere at high temperature (1354 to 1651°C) with both fuel fragments and Zircaloy-clad specimens. These experiments demonstrate that hydrogen production from the Zircaloy/steam reaction will significantly reduce the oxygen potential and subsequent cesium release. An enhancement in the release due to temperature ramp up is considered in this analysis. A trapped fraction correlation has also been developed from other CRL test data.
3. The accuracy of the model has been quantified (mean absolute deviation of 0.11) from a validation set of eight experiments. The present model is also in better agreement, as compared to predictions with the industry-standard CORSOR-M and ORNL release models.

ACKNOWLEDGEMENTS

The authors would like to acknowledge the experimental work performed by the Fission Product Release Group at the CRL.

The experimental work at the CRL was funded by Atomic Energy of Canada Limited, Ontario Hydro, Hydro Quebec and New Brunswick Electric Power Corporation under the CANDU Owner's Group agreement. The work at RMC was supported by the Academic Research Program of the Department of National Defence of Canada (allocation no. 3705-882) and the Natural Sciences and Engineering Research Council of Canada (award no. OGP0155726).

TABLE 1. - MODEL PARAMETERS BASED ON CRL HCE2 TEST CONDITIONS.

Parameter	Fuel Fragment Tests ^(k)			Mini-Element Tests ^(k)		
	HCE2-CF2	HCE2-CF3	HCE2-CF1	HCE2-CM2	HCE2-CM6	HCE2-CM1
Pre-Test Conditions:						
Fuel Type	Bruce-type ^(l)	Bruce-type ^(l)	Bruce-type ^(l)	Bruce-type ^(l)	Bruce-type ^(l)	Bruce-type ^(l)
Element Identity	AC-19	AC-19	AC-19	AC-19	AC-19	AC-19
Burnup (MWh/kgU)	457.2	457.2	457.2	457.2	457.2	457.2
Test Description:						
Fuel Specimen	UO ₂ chips	UO ₂ chips	UO ₂ chips	UO ₂ /Zr-4 ⁽ⁿ⁾	UO ₂ /Zr-4 ⁽ⁿ⁾	UO ₂ /Zr-4 ⁽ⁿ⁾
Enrichment (wt% ²³⁵ U in U)	1.38	1.38	1.38	1.38	1.38	1.38
Specimen Weight (g)	0.566	0.534	0.460	14.696 ^(o)	16.890 ^(o)	16.469 ^(o)
Number of Fragments ^(a)	3	3	2	—	—	—
Fuel Length (mm) ^(b)	—	—	—	9	11	10
Grain Radius (μm)	3.5 ^(m)	3.5 ^(m)	3.5 ^(m)	6.5 ^(p)	6.5 ^(p)	6.5 ^(p)
Temperature (°C)	1354	1504	1639	1368	1496	1651
Environment ^(c)	Ar/2%-H ₂ , steam	Ar/2%-H ₂ , steam	Ar/2%-H ₂ , steam	Ar/2%-H ₂ , steam	Ar/2%-H ₂ , steam	Ar/2%-H ₂ , steam
Modelling Analysis:						
Gap Inventory ^(q)	—	—	—	0.15	0.15	0.15
Equilibrium x _e (experiment) ^(r)	0.17	0.16	0.15	—	—	—
Equilibrium x _e (model) ^(r)	0.20	0.19	0.17	—	—	—
End-of-Test x (experiment) ^(s)	0.18	0.16	0.15	0.18	0.16	0.15
End-of-Test x (model) ^(s)	0.20	0.19	0.17	0.17	0.19	0.17
S/V Ratio (m ⁻¹) (Fitted) ^(j)	2.10×10 ⁴	4.67×10 ⁴	1.55×10 ⁴	—	—	—
S/V Ratio (m ⁻¹) (Model) ^(j)	2.07×10 ⁴	2.11×10 ⁴	1.29×10 ⁴	1.65×10 ³	1.53×10 ³	1.59×10 ³
Model Parameters: Temperature Ramp ^(k) : E _r = 1.78×10 ² (s/K)						
Inert Atmosphere ^(c) : D _{ox} = 7.6×10 ⁻¹⁰ (m ² /s) Q _{ox} = 7.0×10 ⁴ (cal/mol)						
Steam Atmosphere ^(c) : D _{ox} = 2.22×10 ⁻⁸ (m ² /s) Q _{ox} = 4.02×10 ⁴ (cal/mol)						

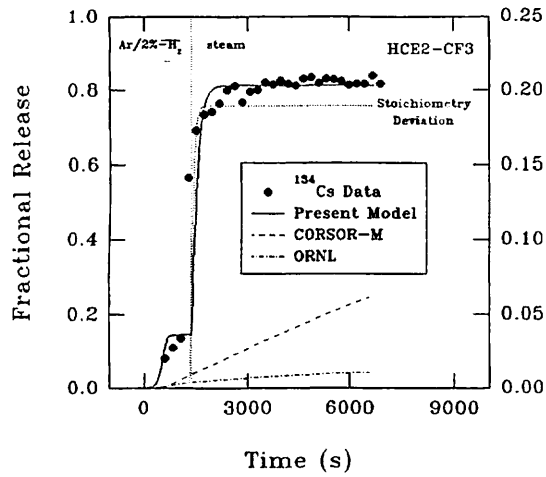
- (a) Applicable to fuel fragment tests only.
- (b) Applicable to mini-element tests only.
- (c) For standard temperature and pressure conditions.
- (d) Fraction of ¹³⁴Cs in the fuel-to-clad gap (mini-elements only).
- (e) Calculation based on measured p_{ox} data and Blackburn model.
- (f) Calculation assuming oxygen potential for pure steam (Q_r=2) and Blackburn model.
- (g) Calculation based on measured weight gain at end of test.
- (h) Calculation based on measured p_{ox} data followed by pure steam assumption (Q_r=2) and Blackburn model.
- (i) Fit performed on fuel fragments only.
- (j) S/V = 3*(S/V)_{geometric} (assuming cubic geometry for fuel fragment tests).
- (k) Tests are in order of increasing temperature.
- (l) Bruce-type fuel rod irradiated in the NRU reactor (enriched to 1.38 wt% ²³⁵U).
- (m) Range of 2 to 5-μm (peripheral fragments chosen based on high Cs/Rh ratio).
- (n) UO₂ clad in Zircaloy-4 with loose fitting end-caps.
- (o) Includes the weight of the Zircaloy-4 cladding and end-caps.
- (p) Based on volumetric average of as-received, irradiated fuel pellet.
- (q) Determined from a simultaneous fit to all six tests.
- (r) Intrinsic diffusion coefficient as previously determined by Turnbull.
- (s) Determined from a simultaneous fit to all six tests.

TABLE 2. TRAPPED FRACTION BASED ON CRL EXPERIMENTAL DATA.

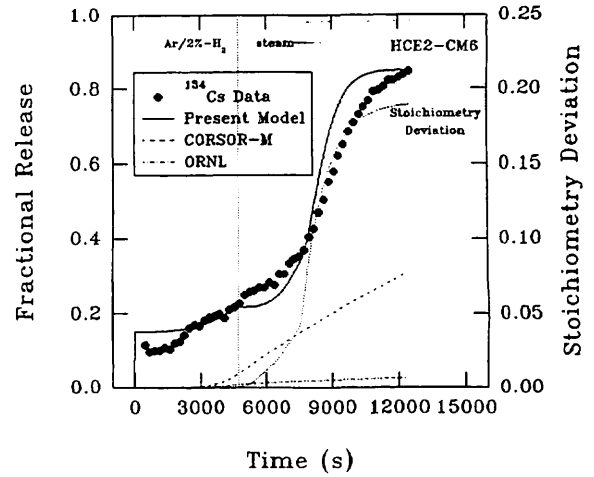
Test	Specimen Type	Temperature ^(b) (°C)	Environment ^(c)	Grain Radius (µm)	Burnup (MWh/kgU)	Trapped Fraction, ζ	
						Measured ^(d)	Model ^(e)
HCE1-M12 ^(a)	mini-element	1599	steam	6.5 ^(d)	457.2	— ^(g)	0.101
HCE1-M13	mini-element	1603	steam	6.5 ^(d)	457.2	0.136	0.101
HCE1-M14	mini-element	1599	steam	6.5 ^(d)	457.2	0.126	0.101
HCE2-CF1	fuel fragment	1639	steam	3.5 ^(d)	457.2	0.201	0.188
HCE2-CF2	fuel fragment	1354	steam	3.5 ^(d)	457.2	0.059	0.188
HCE2-CF3	fuel fragment	1504	steam	3.5 ^(d)	457.2	0.181	0.188
HCE2-CM1	mini-element	1651	steam	6.5 ^(d)	457.2	0.147	0.101
HCE2-CM2	mini-element	1368	steam	6.5 ^(d)	457.2	— ^(g)	0.101
HCE2-CM5	mini-element	1500	steam	6.5 ^(d)	457.2	0.127	0.101
HCE2-CM6	mini-element	1496	steam	6.5 ^(d)	457.2	0.154	0.101
HCE2-CM7	mini-element	1622	steam	6.5 ^(d)	457.2	0.052	0.101
UCE12-T01 ^(a)	fuel fragment	1104	steam	5.0 ^(d)	441	— ^(g)	0.136
UCE12-T03 ^(a)	fuel fragment	1600	Ar/2%-H ₂	3.3 ^(d)	370	— ^(g)	0.246
UCE12-T05	fuel fragment	1553	steam	5.7 ^(d)	370	0.030	0.142
UCE12-T07 ^(a)	fuel fragment	1555	steam	6.7 ^(d)	441	— ^(g)	0.102
UCE12-T08	mini-element	1400	steam	4.3 ^(d)	370	0.039	0.189
UCE12-T09 ^(a)	mini-element	1398	purified Ar	4.3 ^(d)	370	— ^(g)	0.189
UCE12-T10 ^(a)	mini-element	1598	purified Ar	5.5 ^(d)	441	— ^(g)	0.124
UCE12-T11	mini-element	1586	steam	5.5 ^(d)	441	0.243	0.124
UCE12-T13 ^(a)	mini-element	1100	steam	5.5 ^(d)	441	— ^(g)	0.124
UCE12-T17 ^(a)	fuel fragment	1481	steam	4.5 ^(d)	370	— ^(g)	0.180

Trapped Fraction Correlation^(k): $f(t) = \zeta \cdot a \cdot BU$
 $= 300 (\mu\text{m} \cdot \text{MWh/kgU})$

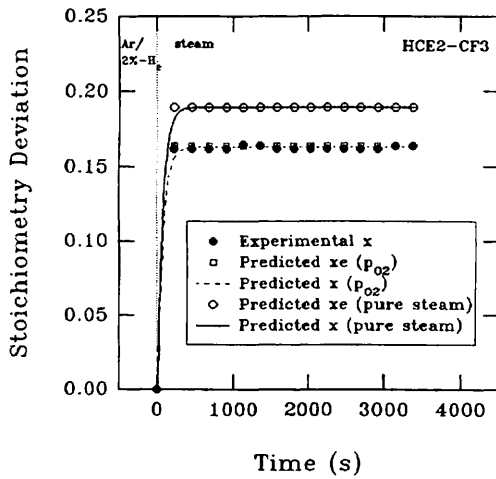
- (a) Test not used in model development or trapped fraction analysis (i.e., model validation test).
(b) Peak test temperature.
(c) For standard temperature and pressure conditions during peak test temperature.
(d) Based on volumetric average of as-received, irradiated fuel pellet.
(e) Range of 2 to 5 µm (peripheral fragments chosen based on a high Cs/Rh ratio).
(f) Determined from post-test ceramographic analysis.
(g) Based on volumetric average from post-test ceramographic analysis.
(h) Determined from end-of-test ¹³⁴Cs release fraction.
(i) End-of-test ¹³⁴Cs release fraction did not reach equilibrium.
(j) Calculation based on trapped fraction correlation.
(k) Value represents average from calculations based on measured trapped fraction.



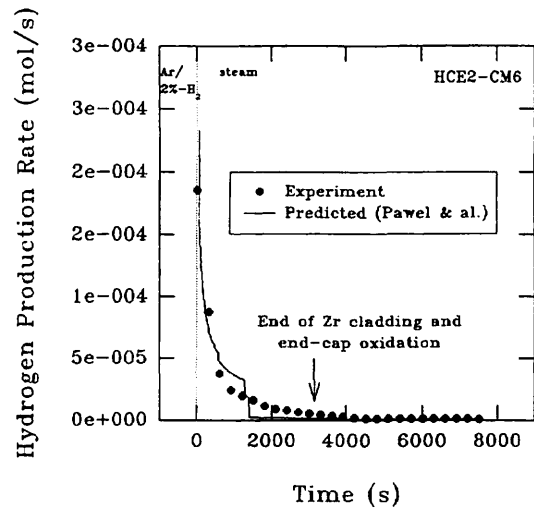
(a)



(b)

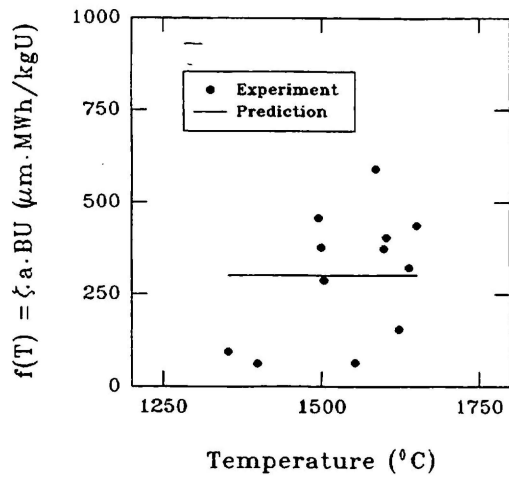


(c)

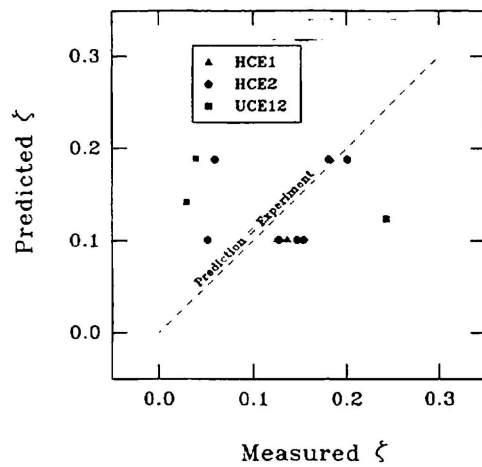


(d)

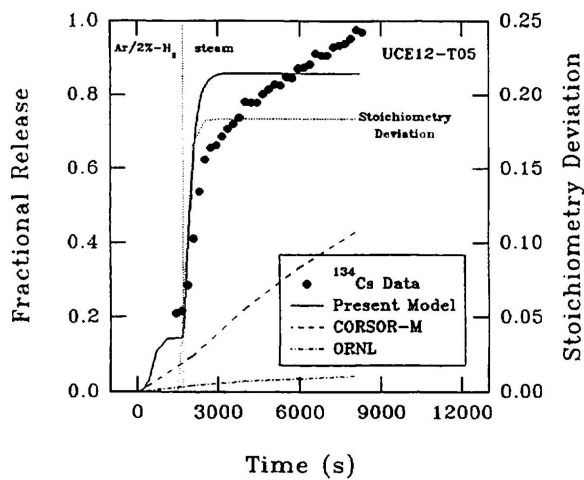
FIGURE 1. COMPARISON OF MODEL PREDICTIONS TO HCE2 EXPERIMENTS. (a) Release fraction for fuel fragment test HCE2-CF3 (1504°C). (b) Release fraction for mini-element test HCE2-CM6 (1496°C). (c) Stoichiometry deviation for fuel fragment test HCE2-CF3. (d) Hydrogen production rate for mini-element test HCE2-CM6.



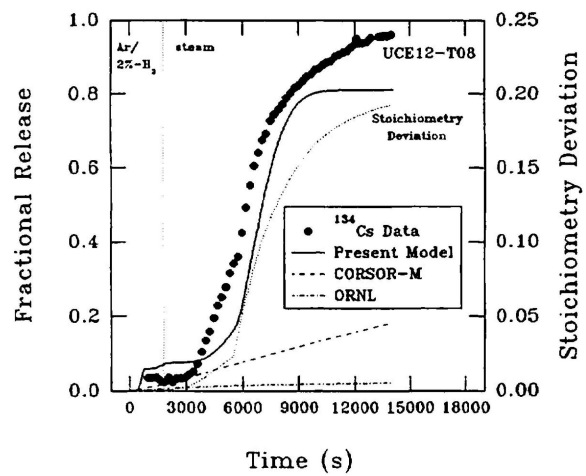
(a)



(b)

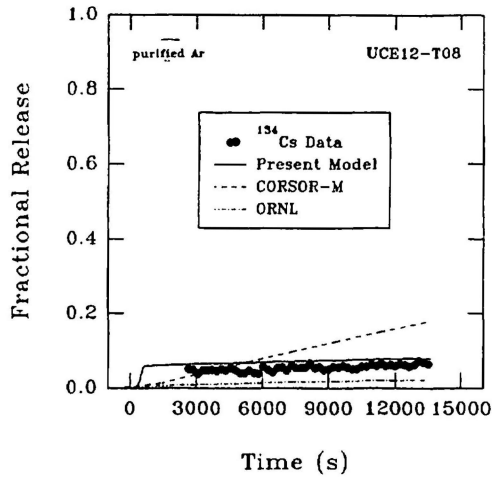


(c)

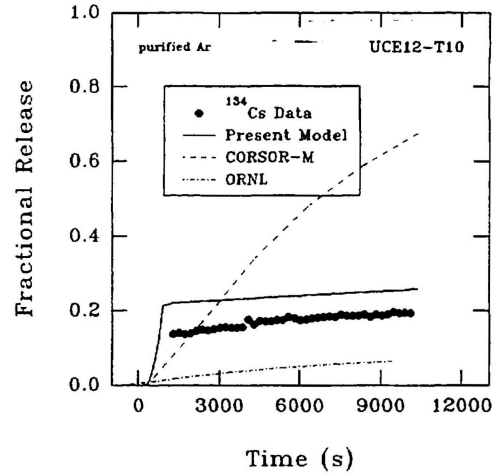


(d)

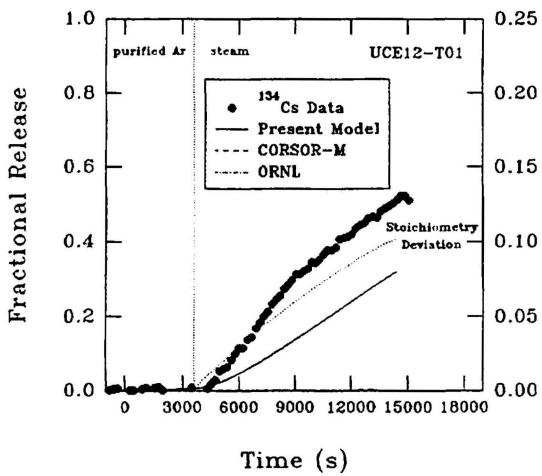
FIGURE 2. TRAPPED FRACTION ANALYSIS. (a) $f(T)$ vs. temperature. (b) Comparison of measured and predicted ζ . (c) Release fraction for fuel fragment test UCE12-T05. (d) Release fraction for mini-element test UCE12-T08.



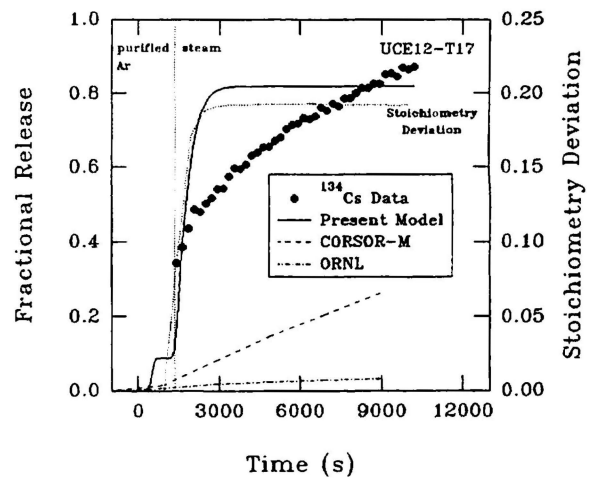
(a)



(b)



(c)



(d)

FIGURE 3. RELEASE FRACTION COMPARISON FOR VALIDATION SET. Mini-element tests (a) UCE12-T08 and (b) T10 in inert (purified argon) atmosphere. Fuel fragment tests (c) UCE12-T01 and (d) T17 in oxidizing (steam) atmosphere.

REFERENCES

- (1) R.S. DICKSON, Z. LIU, D.S. COX, N.A. KELLER, R.F. O'CONNOR AND R.D. BARRAND, "Cesium Release from CANDU Fuel in Argon, Steam and Air: The UCE12 Experiment", Proceedings of the 15th Annual Canadian Nuclear Association Meeting, Montreal, Quebec, Canada, June 1994.
- (2) Z. LIU, D.S. COX, R.S. DICKSON AND P.H. ELDER, "Release of Semi- and Low-Volatile Fission Products from Bare UO_2 Samples during Post-Irradiation Annealing", Proceedings of the 15th Annual Canadian Nuclear Association Meeting, Montreal, Quebec, Canada, June 1994.
- (3) D.S. COX, Z. LIU, R.S. DICKSON AND P.H. ELDER, "Fission-Product Releases during Post-Irradiation Annealing of High-Burnup CANDU Fuel", Proceedings of the Third International Conference on CANDU Fuel, Pembroke, Ontario, Canada, October 1992.
- (4) R.S. DICKSON, C.Y. LEE, Z. LIU, C.E.L. HUNT, D.S. COX, N.A. KELLER, R.F. O'CONNOR AND R.D. BARRAND, "Krypton and Cesium Release from UO_2 Mini-Element Specimens in Air, Steam and Argon Atmospheres at 1100-1600°C: UCE12 Data and Analysis Report", Atomic Energy of Canada Limited Report, AECL, COG-92-331, March 1994.
- (5) D.S. COX, Z. LIU, P.H. ELDER, C.E.L. HUNT AND V.I. ARIMESCU, "Fission-Product Release Kinetics from CANDU and LWR Fuel During High-Temperature Steam Oxidation Experiments", presented at IAEA Technical Committee Meeting on Fission Gas Release and Fuel Rod Chemistry Related to Extended Burnup, Pembroke, Ontario, Canada, 28 April - 1 May 1992.
- (6) B.J. LEWIS, F.C. IGLESIAS, C.E.L. HUNT AND D.S. COX, "Release Kinetics of Volatile Fission Products Under Severe Accident Conditions", Nucl. Technol. 99 (1992) 330.
- (7) B.J. LEWIS, D.S. COX AND F.C. IGLESIAS, "A Kinetic Model for Fission-Product Release and Fuel Oxidation Behaviour for Zircaloy-Clad Fuel Elements Under Reactor Accident Conditions", J. Nucl. Mater. 207 (1993) 228.
- (8) D.S. COX, R.F. O'CONNOR AND W.W. SMELTZER, "Measurement of Oxidation/Reduction Kinetics to 2100°C Using Non-Contact Solid-State Electrolytes", Solid State Ionics 53-56 (1992) 238.
- (9) D.S. COX, F.C. IGLESIAS, C.E.L. HUNT, N.A. KELLER, R.D. BARRAND, J.R. MITCHELL AND R.F. O'CONNOR, "Oxidation of UO_2 in Air and Steam with Relevance to Fission Product Releases", Proc. Symp. Chemical Phenomenon Associated with Radioactivity During Severe Nuclear Plant Accidents, Anaheim, California, 9-12 September 1986, NUREG/CP-0078, p. 2, U.S. Nuclear Regulatory Commission (1986).
- (10) A.C. HARNDEN-GILLIS, B.J. LEWIS, W.S. ANDREWS, P.L. PURDY, M.F. OSBORNE AND R.A. LORENZ, "Modelling of Cesium Release from Light Water Reactor Fuel Under Severe Accident Conditions", Nucl. Technol. 109 (1995) 39.
- (11) J. CRANK, "The Mathematics of Diffusion", 2nd ed., p. 4, Oxford University Press, London (1975).
- (12) H. MATZKE, "Gas Release Mechanisms in UO_2 - A Critical Review", Radiat. Eff. 53 (1980) 219.

- (13) R.W. GRIMES AND C.R. CATLOW, "The Stability of Fission Products in Uranium Dioxide", *Philos. Trans. R. Soc. London Ser. A*, 335 (1991) 609.
- (14) A.B. LIDIARD, "Self Diffusion of Uranium in UO_2 ", *J. Nucl. Mater.* 19 (1966) 106.
- (15) J.C. KILLEEN AND J.A. TURNBULL, "An Experimental and Theoretical Treatment of the Release of ^{85}Kr from Hyperstoichiometric Uranium Dioxide", *Proc. Workshop on the Chemical Reactivity of Oxide Fuel and Fission Product Release*, Gloucestershire, England, 7-9 April, 1987, p. 387, Central Electricity Generating Board.
- (16) J.A. TURNBULL, R.J. WHITE AND C. WISE, "The Diffusion Coefficient for Fission Gas Atoms in Uranium Dioxide", *Proc. IAEA Technical Committee Meeting on Water Reactor Fuel Element Computer Modelling in Steady-State, Transient and Accident Conditions*, Preston, England, 18-22 September, 1988, International Atomic Energy Agency (1988).
- (17) C.F. GERALD AND P.O. WHEATLY, "Applied Numerical Analysis", 4th ed., p. 15, Addison-Wesley Publishing Company, New York (1989).
- (18) D.R. OLANDER, "Oxidation of UO_2 by High-Pressure Steam", *Nucl. Technol.* 74 (1986) 215.
- (19) P.E. BLACKBURN, "Oxygen Pressures over Fast Breeder Reactor Fuel (I) A Model for UO_{2+x} ", *J. Nucl. Mater.* 46 (1973) 244.
- (20) R.E. CARTER AND K.W. LAY, "Surface-Controlled Oxidation-Reduction of UO_2 ", *J. Nucl. Mater.* 36 (1970) 77.
- (21) J.A. MEACHEN, "Oxygen Diffusion in Uranium Dioxide: A Review", *Nucl. Energy* 28 (1989) 221.
- (22) D.S. COX, F.C. IGLESIAS, C.E.L. HUNT, R.F. O'CONNOR AND R.D. BARRAND, "High-Temperature Oxidation Behaviour of UO_2 in Air and Steam", *Proc. Int. Symp. High-Temperature Oxidation and Sulphidation Processes*, Hamilton, Ontario, Canada, 26-30 August, 1990.
- (23) J. ABREFAH, A. DE AGUIAR BRAID, W. WANG, Y. KHALIL AND D.R. OLANDER, "High Temperature Oxidation of UO_2 in Steam-Hydrogen Mixtures", *J. Nucl. Mater.* 208 (1994) 98.
- (24) J.A. TURNBULL, C.A. FRISKNEY, J.R. FINDLAY, F.A. JOHNSON AND A.J. WALTER, "The Diffusion Coefficients of Gaseous and Volatile Species During the Irradiation of Uranium Dioxide", *J. Nucl. Mater.* 107 (1982) 168.
- (25) K. UNE AND S. KASHIBE, "Fission Gas Release During Postirradiation Annealing of UO_2 -2 wt% Gd_2O_3 Fuels", *J. Nucl. Mater.* 189 (1992) 210.
- (26) J. KUO, S. MCDONALD AND E. FOX, "SigmaPlot Scientific Graphing Software", User's Manual, Version 5.00, Jandel Scientific (1992).
- (27) M.J. NOTLEY, "ELESIM: A Computer Code for Predicting the Performance of Nuclear Fuel Elements", *Nucl. Technol.* 44 (1979) 445.
- (28) T. YAMASHITA, "Steam Oxidation of Zircaloy Cladding in the ORNL Fission Product Release Tests", *NUREG/CR-4777 (ORNL/TM-10272)*, Oak Ridge National Laboratory (1988).

- (29) R.E. PAWEL, J.V. CATHCART AND R.A. MCKEE, "The Kinetics of Oxidation of Zircaloy-4 in Steam at High Temperatures", J. Electrochem. Soc. 126 (1979) 1105.
- (30) M.J. NOTLEY, "FP Release Modelling and Validation", Meeting note 4204176, Commissariat a l'Energie Atomique - Cadarache, p. 6, 31 January 1995.
- (31) D.R. OLANDER, "Fundamental Aspects of Nuclear Reactor Fuel Elements", TID-267711-P1, U.S. Department of Commerce, National Technical Information Service, p. 203 (1976).
- (32) M.R. KUHLMAN, D.J. LEHMICKE AND R.O. MEYER, "CORSOR User's Manual", Battelle's Columbus Laboratories, NUREG/CR-4173, March 1985.
- (33) M.F. OSBORNE AND R.A. LORENZ, "ORNL Studies of Fission Product Release Under LWR Severe Accident Conditions", Nucl. Safety 33 (1992) 344.